OPEN

PRS GLOBAL OPEN

EXPERIMENTAL

Plasticity of Unmyelinated Fibers in a Side-to-end Tubulization Model

Vânia Tognon-Miguel, MS*
Adriana H. Nascimento-Elias, PhD*†
Maria C. L. Schiavoni, MS*
Amilton A. Barreira, MD, PhD*

Background: Histomorphometric studies of unmyelinated fibers of the rat fibular nerves are uncommon, and side-to-end neurorrhaphy studies using the fibular nerve investigate primarily motor fibers. We investigated side-to-end tubulization (SET) technique, in which occurs collateral sprouting from the intact donor nerve fibers to the distal stump of receptor nerve, with muscle reinnervation and functional rehabilitation, to assess whether there is a successful growth of unmyelinated fibers in this model.
Methods: Adult Wistar rats fibular nerves were sectioned to create a 5-mm gap. A 6-mm silicone tube was attached between a side of the intact tibial nerve and the sectioned fibular nerve distal stump (SET group), with the left fibular nerve as normal (sham group). Seventy days postsurgery, unmyelinated fibers from the distal segment of the fibular nerve were quantified using light and transmission electron microscopy and their diameters were measured.
Results: The number of unmyelinated fibers was similar between sham (1,882±270.9) and SET (2,012±1,060.8), but axons density was significantly greater in the SET (18,733.3±5,668.6) than sham (13,935.0±1,875.8). Additionally, the axonal diameters differed significantly between groups with mean measures in sham (0.968±0.10) > SET (0.648±0.08).
Conclusions: Unmyelinated fiber growth occurred even with a 5-mm distance between the donor and receptor nerves, reaching similar axonal number to the normal nerve, demonstrating that the SET is a reliable technique that can promote a remarkable plasticity of unmyelinated axons. *(Plast Reconstr Surg Glob Open 2019;7:e1993; doi: 10.1097/GOX.0000000000001993; Published online 9 January 2019.)*

INTRODUCTION

There are few morphological and morphometric studies of unmyelinated nerve fibers, despite their being widely distributed and processing important sensory and autonomic information.[1,2] Unmyelinated fibers are significant components of both the autonomic nervous system and sensory afferents, transmitting information from cutaneous and visceral areas to the central nervous system, and are primarily responsible for tactile, thermal, and pain sensations.[3–7] Regeneration of unmyelinated fibers leading to reinnervation is important because those sensation modalities are crucial for skin preservation, preventing contact pressure ulcers (bedsores) formation in man,[8–11] and also autophagy or autotomy in rats.[12,13] Previous studies of nerve regeneration using side-to-end neurorrhaphy (SEN) in man[14–20] and in rats[21–27] or a variant technique using tubular conduits in rats[28–37] have assessed mostly myelinated fibers. These studies revealed that, in the most widely used experimental model of SEN, suturing the distal stump of the fibular nerve to the lateral portion of the tibial nerve is typically performed followed by the epi-perineurial window. Previous studies quantifying unmyelinated fibers of the fibular nerve have yielded conflicting results concerning axonal number.[2] Research published by Kovacic et al.[38–42] demonstrated growth of sural nerve unmyelinated fibers to the injured fibular nerve using SEN.

*From the *Department of Neurosciences and Behavioral Sciences, Medical School of Ribeirão Preto, University of São Paulo, Ribeirão Preto, SP, Brazil; and †Department of Biomechanics, Medicine and Rehabilitation of the Locomotor System, Medical School of Ribeirão Preto, University of São Paulo, Ribeirão Preto, SP, Brazil.*
Received for publication April 24, 2018; accepted September 14, 2018.
Partial results of this study were presented at the Peripheral Nerve Society Meeting 2015, Quebec City, Canada, and at the 12th International Microsurgery Symposium 2014, Botucatu, Brazil.
Supported by grants from Fundação de Amparo à Pesquisa do Estado de São Paulo (FAPESP – 2012/11012–7), CAPES (Coordenação de Aperfeiçoamento de Pessoal de Nível Superior), Conselho Nacional de Desenvolvimento Cientifico e Tecnológico (CNPq – 141524/2015-4), and FAEPA (Fundação de Apoio ao Ensino, Pesquisa e à Assistência do Hospital das Clínicas da Universidade de São Paulo).

DOI: 10.1097/GOX.0000000000001993

Disclosure: *The authors have no financial interest to declare in relation to the content of this article. The Article Processing Charge was paid in part by the Coordenação de Aperfeiçoamento de Pessoal de Nível Superior - Brasil (CAPES) - Finance Code 001.*

The present study assessed whether intact tibial nerves are successful unmyelinated fiber donors to the sectioned fibular nerves using SEN with a gap, using a rigid silicone tube interposed between the lateral portion of the intact tibial nerve (without an epi-perineurial window) and the distal stump of the fibular nerve. We report here that the side-to-end tubulization (SET) is a reliable reconstructive technique and can promote a remarkable plasticity of unmyelinated axons.

MATERIALS AND METHODS

Animals and Surgical Procedures

All experiments were conducted with approval from the Animal Experimentation Ethics Committee at the Medical School of Ribeirão Preto, University of São Paulo (protocol number 024/2010). Ten 7- to 8-week-old female Wistar rats (250–300 g) were used. Food and water were provided ad libitum. The animals were anesthetized using ketamine chloridrate (75 mg/kg) and xylazine (15 mg/kg), administered intraperitoneally. The right sciatic nerve and its branches were exposed, and the common fibular nerve was sectioned 3 mm from its origin. The proximal stump was then buried and sutured into the adjacent musculature. A silicone tube (6 mm in length × 1.47 mm inner diameter × 1.96 mm outer diameter; DeganiaSilicone Ltd., Israel) was attached to the adjacent lateral portion of the intact tibial nerve, and the distal stump of the common fibular nerve was sutured to the other end of the tube. All sutures were made with 10-0 nylon (Bioline) sutures. This procedure is referred to as SET (Fig. 1). The distal segment of the left common fibular nerve was used as normal (sham group). Fibular nerves were fixed in situ using 2% glutaraldehyde in 0.025 M, pH 7.4 sodium cacodylate buffer and dissected 70 days after tubulization. After removal of the nerves, the animals were euthanized using large quantities of the previously described anesthetics.

Histological Evaluation and Morphometry

The distal segment of the fibular nerve was sectioned 3 mm from the distal end of the tube, immersed in a 2% glutaraldehyde solution (48 h at 4°C), washed with sodium cacodylate buffer, postfixed in 1% osmium tetroxide, progressively dehydrated, and embedded in epoxy resin (Epon 812, Electron Microscopy Sciences, Hatfield, PA).

Samples were then cut into 0.5-µm-thick sections using a microtome (MT 6000XL- RMC, Boeckeler Instruments Inc., Tucson, AZ), stained with toluidine blue, and mounted using Entellan (Sigma-Aldrich Co., Darmstadt, Germany) for analyses using light microscopy. Details of the methods have previously been published.[2]

Transmission Electron Microscopy Procedures

An ultramicrotome (Carl Zeiss, model G/214711) was used to cut the plastic embedded blocks into 80-nm-thick sections, which were placed on oval grids covered with 5% Formvar film (Formvar solution in ethylene dichloride, Electron Microscopy Sciences Inc., Hatfield, PA) and stained with 5% uranyl acetate and 0.5% lead citrate.

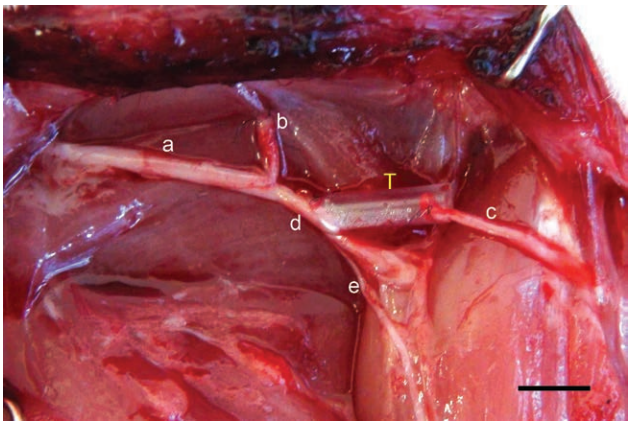

Fig. 1. SET in the right rat fibular nerve immediately after surgery, using a 6-mm silicone tube (T). A 5-mm segment was removed between the nerve stumps. (a) Sciatic nerve, (b) proximal stump of the common fibular nerve, (c) distal stump of the common fibular nerve, (d) tibial nerve, (e) sural nerve. Bar = 3 mm.

The digitalization was obtained using a transmission electron microscope (JEM-100CXII, JEOL Ltd., Tokyo, Japan) equipped with a digital camera (Hamamatsu ORCA-HR, model C4742-51- 12HR). Twenty nerves were assessed, 10 of each group. The cross-sectional fascicular area of the nerve was completely scanned, and images of the endoneurial content were obtained. Sequential photomicrographs were manually collected at 14,000× magnification while scanning occurred. We scanned means of 62% and 76% of the fascicle area from the sham group and the SET group, respectively. Each digital image obtained from the microscopic fields was 14.0 µm wide × 14.0 µm high and 1,024×1,024 pixels in tagged image file format. All images were analyzed. Owing to variability in the fascicular area,[2] we obtained a mean of 413 images per nerve.

Assessment of Unmyelinated Axons

Unmyelinated fibers and their axonal area were measured. The total number of axons, axonal density (axons/mm2), and the minimum axonal diameter (µm) were measured using ImageJ 1.47 software (National Institutes of Health, Bethesda, MD), as described above. Unmyelinated axons were identified using established criteria,[43] as follows: (1) circular or oval profile; (2) surrounded by Schwann cell cytoplasm forming mesaxons; (3) axoplasm that was clearer than the cytoplasm of the respective Schwann cell; (4) clustering into "units," which had a direct relationship with Schwann cells; and (5) basal lamina externally surrounding each fiber unit consisting of Schwann cells and axons.

Only regular sectioned fibers and axons with circular shapes were reported. Measurements of the internal fascicular area (mm2) were similar to those obtained in semithin sections; since semithin sections produced clearer images, we used them to measure the fascicular areas.[2]

Statistical Analyses

Student's *t* tests were used to compare frequencies and percentage minimum diameter data between groups, and

a $\chi 2$ test was used to compare frequencies of fiber diameters between groups. All values are reported as the mean ± SDs. Data were analyzed using SPSS v.17.0 (SPSS Inc., Chicago, Ill.) statistical software. Differences were considered significant when $P \leq 0.05$.

RESULTS

Seventy days after tubulization, connections between the nerve stumps occurred in all animals of the SET group, and the macroscopic aspects of the regenerated area appeared similar to normal fibular nerves (Fig. 2). In 5 of the 10 animals, the fascicular area of regenerated nerves was lower than that of normal nerves (Fig. 3A), whereas the other five animals had fascicular areas similar to normals. The perineurium, which was composed of one layer in the normal fibular nerve, had 5 layers in the SET group, as shown in Figure 3B. Myelinated and unmyelinated fibers, Schwann cell nuclei, endothelial cells, and mast cells were identified in all samples. However, these features were observed in greater numbers in regenerated nerves than in normals. The unmyelinated fibers were similar to normal nerve fibers, and usually consisted of a few axons, with considerable variability in both area and circularity. The unmyelinated axons had greater variation in their minimum diameters and there were a greater number of these axons in the SET group than in the sham group (Fig. 4A). Three nerves from the SET group showed endoneurial content predominantly populated by collagen fibers, with only a few myelinated fibers, unmyelinated fibers, and other cell types (Fig. 4B). However, the number of unmyelinated fibers was significantly greater in the SET group than in the distal contralateral fibular nerve (Table 1). Additionally, the variability among nerves was greater in the SET group. The median number of axons in normal nerves was 1,987.5, whereas in the SET group, the median was 1,349.5.

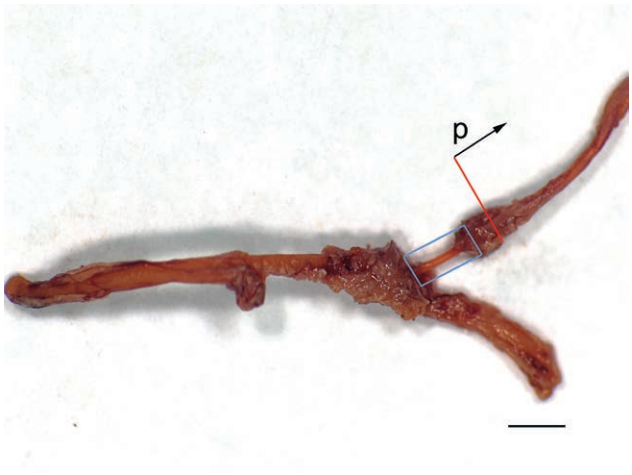

Fig. 2. Nerve segment from the right sciatic SET group, with branches. The blue rectangle represents the position of the silicone tube, with the regeneration cable inside. The red line represents the analysis site, which was 3 mm from the end of the silicone tube. The dashed arrow in black represents the nerve segment designed for proximal inclusion to the enclosing block (p). Bar = 5 mm.

The mean internal fascicular areas, number of axons, minimum axonal diameters, and axonal densities of the sham and SET groups are given in Table 1. The greater density of unmyelinated fibers in the SET group is explained by reduced fascicular area and increased variability in the number of unmyelinated axons. Figure 5 presents the frequency distribution for minimum axonal diameter in both groups. The axon diameters of the normal fibular nerve ranged from 0.2 to 2.8 µm. The minimum diameter of axons in the SET group ranged from 0.2 to 2.6 µm. There were more unmyelinated axons between 1.0 and 1.2 µm in the sham group, whereas there were more axons with minimum diameters between 0.4 and 0.6 µm in the SET group (Fig. 5).

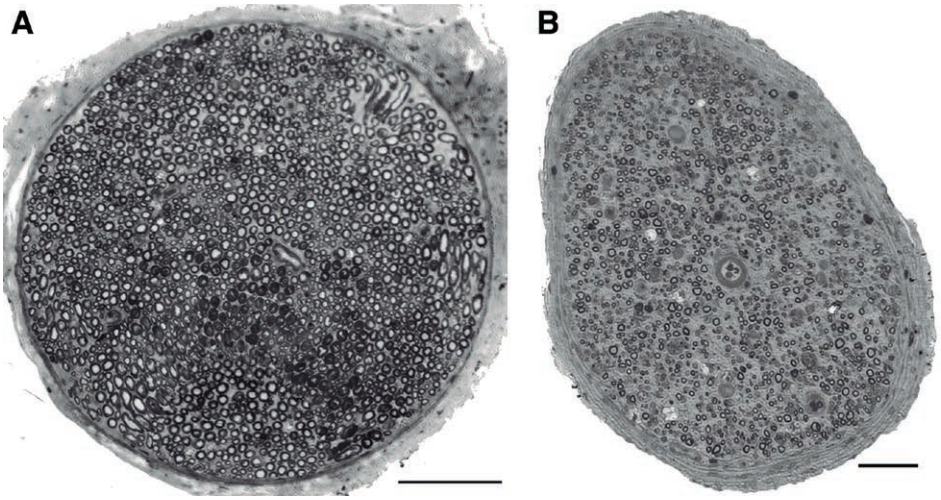

Fig. 3. Photomicrographs of the fascicular areas of the distal segments from normal common fibular nerves and from partially reconstructed nerves 70 days after surgery. Note the difference in the size of the fascicular area between groups. Panel B shows a perineurium constituted of 5 layers, which is in contrast to 1 layer in the normal fibular nerve. A, Normal distal fibular nerve (sham group). B, Reconstructed distal fibular nerve 70 days after SET group, at the same level as the image in A. Semithin sections (0.5 µm). Toluidine blue. Bar = 100 µm.

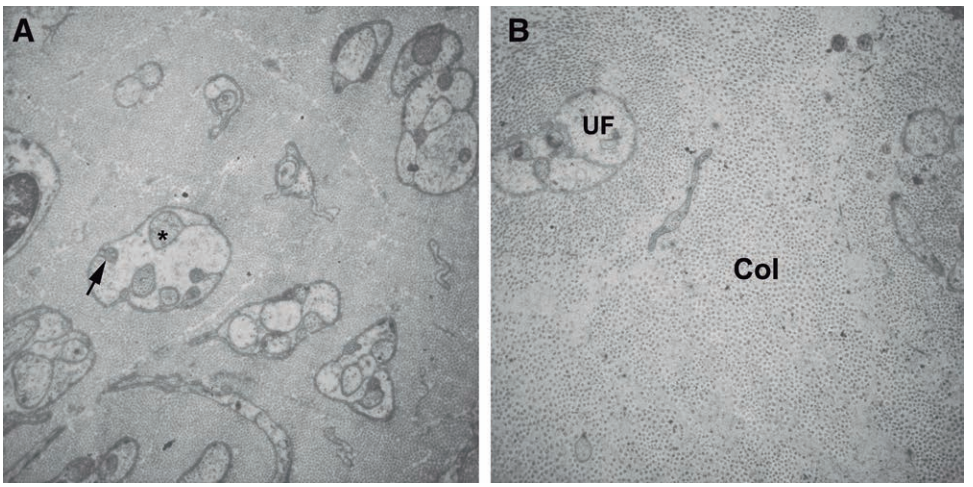

Fig. 4. Electron micrographs of cross-sections of distal segments from 2 common fibular nerves from the SET group. A, There are a large number of unmyelinated fibers; however, Schwann cell units are associated with one or few axons. Most axons have small diameters compared with the sham group. However, the variability in axonal diameter was often high within the same unit (arrow = unmyelinated axon of smaller caliber; * = unmyelinated axon of larger caliber). B, Predominance of collagen fibers (Col) involving an unmyelinated fiber (UF) with 3 unmyelinated axons of small diameters. Transmission electron microscopy—14.000×. Bar = 2 µm.

Table 1. Morphometric Parameters

Group	Nerve Area (mm²)	No. Axons	Minimum Axonal Diameter (µm)	Density of Axons (Axons/mm²)
Sham (n = 10)	0.13 ± 0.02	1,882 ± 270.9	0.968 ± 0.10*	13,935.0 ± 1,875.8
SET (n = 10)	0.11 ± 0.04	2,012 ± 1,060.8	0.648 ± 0.08	18,733.3 ± 5,668.6*

Data are presented as mean ± SD, except for number of axons.
*Indicates a significant difference between the sham group and experimental group (SET; $P \leq 0.05$; Student's t test).

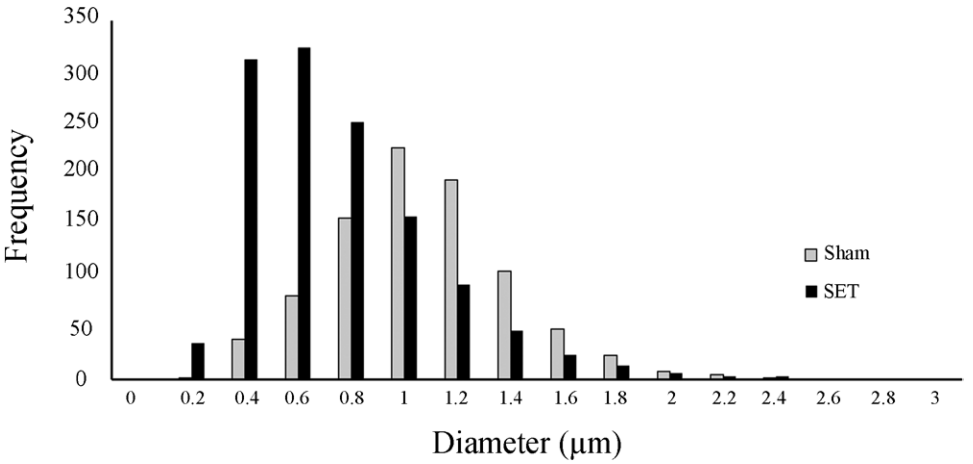

Fig. 5. Histogram of axon numbers in the left normal distal fibular nerve (normal group = sham) compared with the right distal fibular nerve reconstructed using SET. There is a shift to the left, indicating reduced diameters of unmyelinated fibers in the SET group, particularly in the 0.4–0.6 µm diameter range.

DISCUSSION

The unmyelinated fibers in this study traversed the 5-mm gap created by SET and reached the distal segment of the fibular nerve. A literature search did not reveal previous experimental studies on unmyelinated fibers with SEN, either with or without tubulization from the normal tibial nerve to the fibular stump of a previously divided fibular nerve, which is the most common experimental model for SEN. We conducted tubulization using a rigid silicon tube with the intention that future studies can build on our work and observe the actions of nerve growth promoters. Although both rigid and nonrigid tubes have been

used in previous studies, they have not previously been used in studies of unmyelinated fibers with SEN.[33,34,37]

The study evidence a difference between fascicular areas in half of the SET group that was lower than in the sham group. At this time, 70 days post surgery, data describing nerves area in current developing at axonal phase, referring to the regenerating process not completed yet.[44] Data about perineurial layers difference between groups support this report, supposing that at the final regeneration process, the perineurial layers will be condensed in a unique multilayered cellular membrane.[45]

Although some previous studies have demonstrated that a perineurial window induces greater collateral fibers growth,[46,47] we chose not to use an epi-perineurial window, due to work of Viterbo et al.[24] not revealing any differences between end-to-side neurorrhaphies with and without perineurial window concerning the morphological features. Our findings demonstrate profuse growth of unmyelinated fibers, which were often more numerous than the average number of fibers in normal nerves. Future studies are needed to compare the growth of sensory and motor fibers this tubulization experimental model.

Unmyelinated fibers in the fibular nerve are generally classified as 73% afferent (sensory) and 27% efferent (sympathetic).[48] The majority of quantitative studies of unmyelinated fibers in peripheral nerves are conducted on the sural nerve.

Unmyelinated fibers or C fibers carry thermal and pain sensations; therefore, the sural nerve is commonly studied because 92% of its axons conduct sensory information.[6] A previous SEN study used the sural nerve as the donor nerve at the distal stump of the fibular nerve and evaluated myelinated and unmyelinated fibers. After 56 days, there were <800 axons observed 4 mm from the neurorrhaphy site in the fibular nerve.[39] This SEN procedure was conducted without tubulization of the sural-fibular nerves; therefore, more profuse growth of unmyelinated fibers was expected. In the present study, we found a mean of 2,011 unmyelinated axons (median = 1,349.5) in the distal end of the tubulized fibular nerve. Despite the prominent axonal growth in our research, even applying a tubular scaffold on a gap comparing with the study with SEN above cited, we can't assert that tibial nerve are better donor nerve than sural nerve, because the experimental models approaches are different.

We studied adult rats (130 days) because the sciatic nerve has more axons during development than in adult rats. Axons are eliminated during the maturation process.[49] Furthermore, by using the tibial nerve as a source of unmyelinated fibers, we avoided the possibility of transitory sprouts that might experience further elimination, because axon growth appears to be stable in the tibial nerve. After axotomy or nerve crush injury in adult rats, the number of unmyelinated axons transiently increases before returning to normal numbers.[50] A previous experiment by Kovacic found that coaptating the rat sural nerve as a lateral donor to the fibular nerve resulted in stabilization of unmyelinated fiber growth at 2–4 months after surgery.[39] This leads us to suppose that our research time (70th day) contemplates the same situation.

The majority of the SEN studies in man contemplate the motor function recovery.[14–20,51,52] Although some studies have evaluated sensory recovery after SEN,[53-,57] the thermal, tactile, and pain sensations have not been systematically evaluated and few studies applied appropriate analysis that refers to those kinds of findings.[58–60]

Lack of those modalities of sensations can be potential causes of pressure ulcers and accidental injuries, as occur in some predominantly sensory neuropathies, such as leprosy and hereditary sensory neuropathies. So, it is recommended in the clinical setting, not only a clinical evaluation but a quantitative sensory test evaluation of those sensations of the skin supposedly reinnervated after nerve regeneration surgical procedure.

CONCLUSIONS

The present study demonstrates plasticity of unmyelinated axons with SET, using the tibial nerve as a donor. Long-term studies are needed to study changes in thermal and pain sensation that result from fibular nerve sectioning and to evaluate the stability of the unmyelinated fiber growth accomplished by SET. It is possible and even probable that in SEN without tubulization, even greater fiber growth occurs. The effect of nerve growth enhancers should also be studied, and SET is an appropriate model for these studies.

Amilton Antunes Barreira, MD, PhD
Medical School of Ribeirão Preto
Av. Bandeirantes 3900
CEP 14049–900, Ribeirão Preto
São Paulo, Brazil
E-mail: aabarrei@fmrp.usp.br

ACKNOWLEDGMENTS

The authors thank Mr. Antonio Renato Meirelles e Silva, Mrs. Aracy Edwirges Vieira da Silva Dias, Mrs. Maria Teresa Picinoto Maglia, and Mr. José Augusto Maulin for their technical assistance, as well as Mr. Geraldo Cássio dos Reis for his assistance with the statistical analyses.

REFERENCES

1. Ochoa J. Recognition of unmyelinated fiber disease: morphologic criteria. *Muscle Nerve.* 1978;1:375–387.
2. Tognon-Miguel V, Nascimento-Elias AH, Schiavoni MC, et al. A histomorphometric study of unmyelinated fibers of the fibular nerve in Wistar rats. *Arq Neuropsiquiatr.* 2016;74:367–372.
3. Von Euler C. Differences between autonomic and somatic C fibres to stimulation with constant currents. *Acta Physiol Scand.* 1948;15:93–99.
4. Fernández-Morán H. The submicroscopic organization of vertebrate nerve fibres: an electron microscope study of myelinated and unmyelinated nerve fibres. *Exp Cell Res.* 1952;3:282–359.
5. Elfvin LG. Electron microscopic investigation of the plasma membrane and myelin sheath of autonomic nerve fibers in the cat. *J Ultrastruct Res.* 1961;5:388–407.
6. Swett JE, Torigoe Y, Elie VR, et al. Sensory neurons of the rat sciatic nerve. *Exp Neurol.* 1991;114:82–103.
7. Guyton AC, Hall JE. *Textbook of Medical Physiology.* 11th ed. Philadelphia, Pa.: Elsevier; 2006.
8. Denny-Brown D. Hereditary sensory radicular neuropathy. *J Neurol Neurosurg Psychiatry.* 1951;14:237–252.

9. Dyck PJ. Neuronal atrophy and degeneration predominantly affecting peripheral sensory and autonomic neurons. In: Dyck PJ, Thomas PK, Griffin JW, eds. *Peripheral Neuropathy*. 3rd ed. Philadelphia, Pa.: W.B. Saunders; 1993.
10. Viterbo F, Ripari WT. Nerve grafts prevent paraplegic pressure ulcers. *J Reconstr Microsurg*. 2008;24:251–253.
11. Fridman V, Oaklander AL, David WS, et al. Natural history and biomarkers in hereditary sensory neuropathy type 1. *Muscle Nerve*. 2015;51:489–495.
12. Zeltser R, Beilin B, Zaslansky R, et al. Comparison of autotomy behavior induced in rats by various clinically-used neurectomy methods. *Pain*. 2000;89:19–24.
13. Haselbach D, Raffoul W, Larcher L, et al. Regeneration patterns influence hindlimb automutilation after sciatic nerve repair using stem cells in rats. *Neurosci Lett*. 2016;634:153–159.
14. Viterbo F. A new method for treatment of facial palsy: the cross-face nerve transplantation with end-to-side neurorrhaphy. *Rev Soc Bras Cir Plást Estét Reconstr*. 1993;8:29–35.
15. Sawamura Y, Abe H. Hypoglossal-facial nerve side-to-end anastomosis for preservation of hypoglossal function: results of delayed treatment with a new technique. *J Neurosurg*. 1997;86:203–206.
16. Mennen U. End-to-side nerve suture in the human patient. *Hand Surg*. 1998;3:7–15.
17. Frey M, Giovanoli P, Michaelidou M. Functional upgrading of partially recovered facial palsy by cross-face nerve grafting with distal end-to-side neurorrhaphy. *Plast Reconstr Surg*. 2006;117:597–608.
18. Viterbo F, Romão A, Brock RS, et al. Facial reanimation utilizing combined orthodromic temporalis muscle flap and end-to-side cross-face nerve grafts. *Aesthetic Plast Surg*. 2014;38:788–795.
19. Baltzer H, Woo A, Oh C, et al. Comparison of ulnar intrinsic function following supercharge end-to-side anterior interosseous-to-ulnar motor nerve transfer: a matched cohort study of proximal ulnar nerve injury patients. *Plast Reconstr Surg*. 2016;138:1264–1272.
20. Aboshanif M, Omi E, Suzuki S, et al. Facial nerve neuroma in the geniculate ganglion extending into the internal auditory canal: a case report. *Auris Nasus Larynx*. 2018;45:648–652.
21. Viterbo F, Trindade JC, Hoshino K, et al. Latero-terminal neurorrhaphy without removal of the epineural sheath. Experimental study in rats. *Rev Paul Med*. 1992;110:267–275.
22. Viterbo F, Trindade JC, Hoshino K, et al. Two end-to-side neurorrhaphies and nerve graft with removal of the epineural sheath: experimental study in rats. *Br J Plast Surg*. 1994;47:75–80.
23. Viterbo F, Trindade JC, Hoshino K, et al. End-to-side neurorrhaphy with removal of the epineurial sheath: an experimental study in rats. *Plast Reconstr Surg*. 1994;94:1038–1047.
24. Viterbo F, Teixeira E, Hoshino K, et al. End-to-side neurorrhaphy with and without perineurium. *Sao Paulo Med J*. 1998;116:1808–1814.
25. Kovacic U, Bajrović F, Sketelj J. Recovery of cutaneous pain sensitivity after end-to-side nerve repair in the rat. *J Neurosurg*. 1999;91:857–862.
26. Kovacic U, Cör A, Tomsic M, et al. Which myelinated sensory axons sprout into an end-to-side coapted peripheral nerve in the rat? *Acta Neurochir Suppl*. 2007;100:89–91.
27. Kovačič U, Zele T, Tomšič M, et al. Influence of breaching the connective sheaths of the donor nerve on its myelinated sensory axons and on their sprouting into the end-to-side coapted nerve in the rat. *J Neurotrauma*. 2012;29:2805–2815.
28. Matsumoto M, Hirata H, Nishiyama M, et al. Schwann cells can induce collateral sprouting from intact axons: experimental study of end-to-side neurorrhaphy using a Y-chamber model. *J Reconstr Microsurg*. 1999;15:281–286.
29. Yamauchi T, Maeda M, Tamai S, et al. Collateral sprouting mechanism after end-to-side nerve repair in the rat. *Med Electron Microsc*. 2000;33:151–156.
30. Hayashi A, Yanai A, Komuro Y, et al. Collateral sprouting occurs following end-to-side neurorrhaphy. *Plast Reconstr Surg*. 2004;114:129–137.
31. al-Qattan MM, al-Thunyan A. Variables affecting axonal regeneration following end-to-side neurorrhaphy. *Br J Plast Surg*. 1998;51:238–242.
32. Ulkür E, Yüksel F, Açikel C, et al. Comparison of functional results of nerve graft, vein graft, and vein filled with muscle graft in end-to-side neurorrhaphy. *Microsurgery*. 2003;23:40–48.
33. Gravvanis AI, Karvelas M, Lykoudis E, et al. The use of silicone tubes in end- to-side nerve grafting. An experimental study. *Eur J Plast Surg*. 2003;26:111–115.
34. Gravvanis AI, Lavdas A, Papalois AE, et al. Effect of genetically modified Schwann cells with increased motility in end-to-side nerve grafting. *Microsurgery*. 2005;25:423–432.
35. Akeda K, Hirata H, Matsumoto M, et al. Regenerating axons emerge far proximal to the coaptation site in end-to-side nerve coaptation without a perineurial window using a T-shaped chamber. *Plast Reconstr Surg*. 2006;117:1194–203.
36. Manasseri B, Raimondo S, Geuna S, et al. Ulnar nerve repair by end-to-side neurorrhaphy on the median nerve with interposition of a vein: an experimental study. *Microsurgery*. 2007;27:27–31.
37. Lee BK, Ju YM, Cho JG, et al. End-to-side neurorrhaphy using an electrospun PCL/collagen nerve conduit for complex peripheral motor nerve regeneration. *Biomaterials*. 2012;33:9027–9036.
38. Kovacic U, Sketelj J, Bajrović FF. Sex-related difference in collateral sprouting of nociceptive axons after peripheral nerve injury in the rat. *Exp Neurol*. 2003;184:479–488.
39. Kovacic U, Tomsic M, Sketelj J, et al. Collateral sprouting of sensory axons after end-to-side nerve coaptation—a longitudinal study in the rat. *Exp Neurol*. 2007;203:358–369.
40. Kovacic U, Sketelj J, Bajrović FF. Sex-related differences in recovery of cutaneous nociception after end-to-side nerve repair in the rat. *J Plast Reconstr Aesthet Surg*. 2009;62:806–813.
41. Kovacic U, Sketelj J, Bajrović FF. Effect of aging on recovery of cutaneous nociception after end-to-side nerve repair in the rat. *Ann Plast Surg*. 2009;62:439–445.
42. Kovacic U, Zele T, Mars T, et al. Aging impairs collateral sprouting of nociceptive axons in the rat. *Neurobiol Aging*. 2010;31:339–350.
43. Morris JH, Hudson AR, Weddell G. A study of degeneration and regeneration in the divided rat sciatic nerve based on electron microscopy. II. The development of the "regenerating unit." *Z Zellforsch Mikrosk Anat*. 1972;124:103–130.
44. Seckel BR. Enhancement of peripheral nerve regeneration. *Muscle Nerve*. 1990;13:785–800.
45. Olsson Y, Kristensson K. The perineurium as a diffusion barrier to protein tracers following trauma to nerves. *Acta Neuropathol*. 1973;23:105–111.
46. Noah EM, Williams A, Fortes W, et al. A new animal model to investigate axonal sprouting after end-to-side neurorrhaphy. *J Reconstr Microsurg*. 1997;13:317–325.
47. Walker JC, Brenner MJ, Mackinnon SE, et al. Effect of perineurial window size on nerve regeneration, blood-nerve barrier integrity, and functional recovery. *J Neurotrauma*. 2004;21:217–227.
48. Schmalbruch H. Fiber composition of the rat sciatic nerve. *Anat Rec (Hoboken)*. 1986;215:71–81.
49. Jenq CB, Chung K, Coggeshall RE. Postnatal loss of axons in normal rat sciatic nerve. *J Comp Neurol*. 1986;244:445–450.
50. Bray GM, Aguayo AJ. Regeneration of peripheral unmyelinated nerves. Fate of the axonal sprouts which develop after injury. *J Anat*. 1974;117:517–529.
51. Franciosi LF, Modestti C, Mueller SF. Neurotization of the biceps muscle by end-to-side neurorrhaphy between ulnar and musculocutaneous nerves: a series of five cases. *Ann Hand Surg*. 1998;17:362–367.

52. Haninec P, Mencl L, Kaiser R. End-to-side neurorrhaphy in brachial plexus reconstruction. *J Neurosurg*. 2013;119:689–694.
53. Viterbo F, Palhares A, Franciosi LF. Restoration of sensitivity after removal of the sural nerve. A new application of latero-terminal neurorraphy. *Sao Paulo Med J*. 1994;112:658–660.
54. Frey M, Giovanoli P. End-to-side neurorrhaphy of sensory nerves. *Eur J Plast Surg*. 2003;26:85–88.
55. Voche P, Ouattara D. End-to-side neurorrhaphy for defects of palmar sensory digital nerves. *Br J Plast Surg*. 2005;58: 239–244.
56. Artiaco S, Tos P, Conforti LG, et al. Termino-lateral nerve suture in lesions of the digital nerves: clinical experience and literature review. *J Hand Surg Eur Vol*. 2010;35:109–114.
57. Pomares G, Dap F, Dautel G. Results of primary end-to-side digital nerve neurorrhaphy in eight patients. *J Hand Surg Eur*. 2017;42:861–863.
58. Santamaria E, Wei FC, Chen IH, et al. Sensation recovery on innervated radial forearm flap for hemiglossectomy reconstruction by using different recipient nerves. *Plast Reconstr Surg*. 1999;103:450–457.
59. Landwehrs GM, Brüser P. [Clinical results of terminolateral neurorrhaphy in digital nerves]. *Handchir Mikrochir Plast Chir*. 2008;40:318–321.
60. Hosseinian MA, Gharibi Loron A, Nemati Honar B. Reconstruction of the plantar toe with a distal reverse instep sensory island flap. *Microsurgery*. 2018;38:667–673.